Broadband Cross-Polarized Bowtie Antenna for Breast Cancer Detection

Xing Yun*, Elise C. Fear and Ronald Johnston
Department of Electrical and Computer Engineering, University of Calgary
Calgary, Alberta, Canada T2N 1N4 email: johnston@enel.ucalgary.ca

Introduction

Currently, various approaches to microwave breast cancer detection are being investigated by several research groups [1]. Microwave approaches are expected to provide complementary information to that obtained with mammography, the gold standard method for breast imaging. Microwave images are related to the electrical properties of tissues, and there is some evidence to suggest that a contrast exists between normal healthy breast tissues and malignant tumors. Thorough investigations of the properties of specific normal, malignant and benign tissues are required in order to assess the potential effectiveness of microwave tumor detection. If microwave technology provides the capability to detect only malignancies, then it may assist in the diagnosis of suspicious images on mammograms.

One approach to microwave breast imaging, confocal microwave imaging, was introduced by Hagness and colleagues (e.g. [2]). In [2], cross-polarization and the frequency signatures of tumors were proposed as additional diagnostic tools. Cross-polarization was used to detect tumors axially asymmetric to the antenna structure, and to allow for detection of tumors near the chest wall while rejecting co-polarized reflections. The frequency signatures of various tumor shapes were also examined. The use of polarization and resonant frequencies has also been proposed for ground penetrating radar for object detection (e.g. [3]).

In this paper, we investigate the frequency responses of tumors in a simple breast model using computer simulations. Compared to [2], a different frequency range is investigated (2 to 4.25 GHz rather than 3 to 12 GHz). Also, the influence of a variety of parameters (e.g. tumor shape, size, location and depth) on the frequency response is examined.

Methods

The simulated configuration is shown in Fig. 1. The breast model consists of a homogeneous half-space of fat and a 2 mm thick layer of skin. The space above the antenna is also filled with a lossy substance representing fat. Prolate ellipsoidal or spherical tumors are placed below the antenna. The tumor locations and parameter changes studied are indicated in Table 1. Although this model is extremely simple, it provides initial insights into antenna design requirements and estimates for bounds on detection limits. Simulations are performed with WIPL-D

0-7803-7846-6/03/$17.00 ©2003 IEEE

[4], which combines the method of moments with surface integral equations. One antenna is excited and S_{21} is observed.

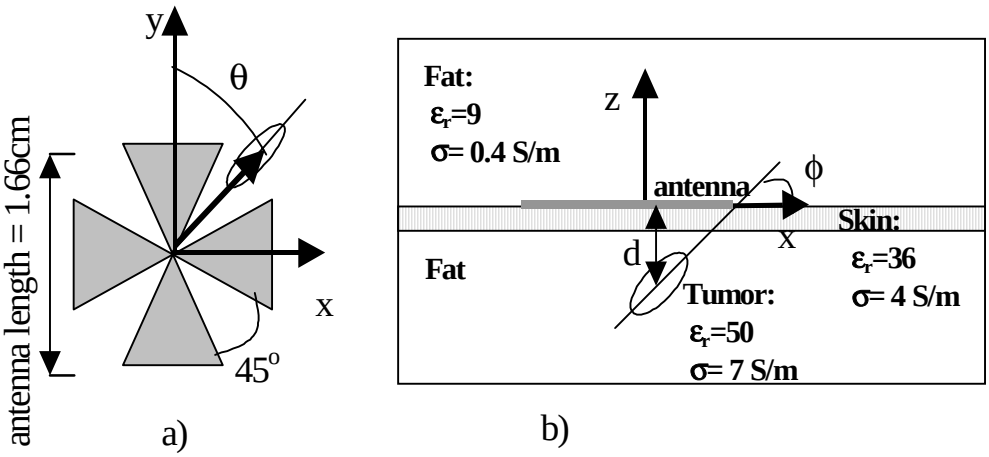

Fig. 1 Simulation configuration. The tumor location is specified by radial distance (r), depth (d), and angles ϕ and θ.

Table 1: Tumor models and locations studied.

Case	Tumor model	Tumor location	Parameter studied
1	Sphere: 5mm diameter	ϕ=0, d=10 mm	Location: - Center of antenna - On y axis with r=5mm – θ=45 °, r=7.07mm
2	Ellipsoid: length=4.8mm, width=1.6mm	θ=45 °, ϕ=0, d=10mm	Location: r=0 mm to r=14.14mm
3	Ellipsoid: length=4.8mm, width=1.6mm	θ=45 °, ϕ=0, r=7.07 mm	Depth: d=10mm to 50 mm
4	Ellipsoid: length/width=3	θ=45 °, ϕ=0 r=7.07 mm, d=50mm	Length: 4.8mm, 3mm, 1.5mm
5	Ellipsoid: length=10mm width=1mm	Center of antenna d=10mm, ϕ=0	θ=0 to 45°
6	Ellipsoid: length=10mm width=1mm	Center of antenna d=10mm, θ=45°	ϕ=0 to 90°

Results and Discussion

The antenna embedded in fatty tissue (without a tumor present) is simulated, and S_{11} is presented in Fig. 2. This indicates that the antenna operates reasonably well from 2 to 4.25 GHz.

To analyze the influence of the skin layer, the tumor described in case 5 is simulated with and without the layer of skin. The amplitude of S_{21} changes,

however the shape of the signal does not. This is expected, as the reflections from the flat skin layer are not observed on S_{21}. Without skin, the maximum increase in amplitude of S_{21} is 1.58dB while the average difference over the frequency range is 0.72dB. To simplify simulations, the skin layer is not considered in following results. Therefore, tumor responses are expected to be smaller than reported due to the effect of the skin.

Changes in response with different tumor locations in the xy plane are examined. Fig. 3 shows the response obtained from a spherical tumor. Limited returns are obtained with the tumor located in the center or on the axis of the antenna. This finding agrees with [2]. Detection of ellipsoidal tumors is examined in Fig. 4. As the tumor moves from the center of the antenna, the magnitude of the response and the curve shape change. For spherical and ellipsoidal tumors in approximately the same location, different frequency responses are observed. Again, this is similar to [2].

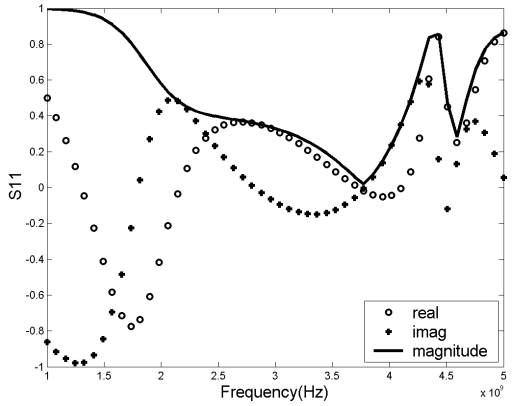

Fig. 2 S_{11} of the antenna.

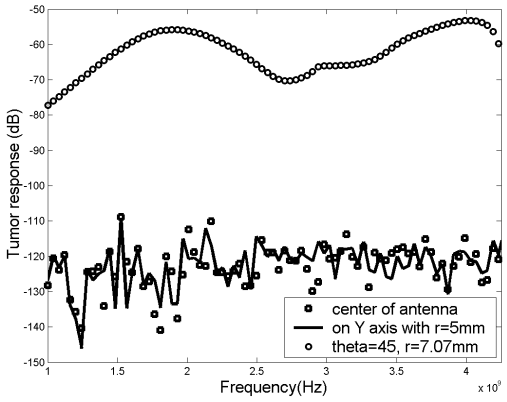

Fig. 3 Change in S_{21} with frequency for a spherical tumor (case 1).

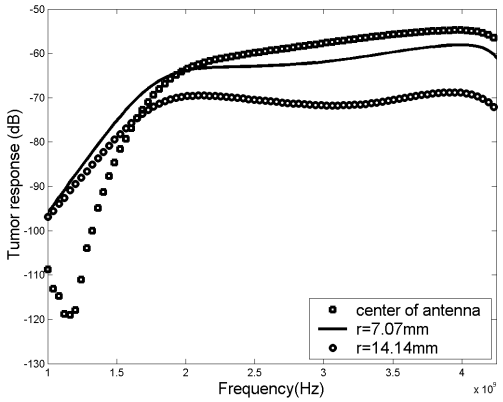

Fig. 4 Change in S_{21} with radial distance (case 2).

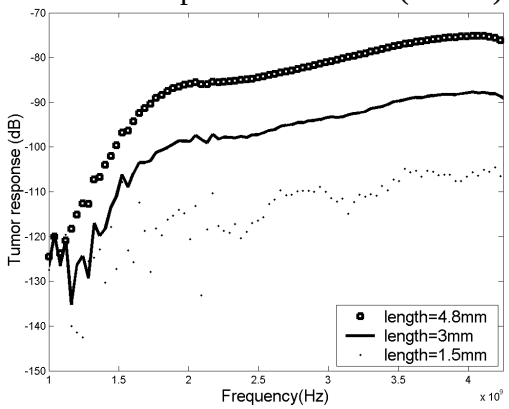

Fig. 5 Change in S_{21} with ellipsoidal tumor size at d=50 mm (case 4).

Next, detection limits are explored by assessing reflections received from deeper and smaller tumors. Case 3 examines the influence of depth on reflections from an ellipsoidal tumor. The curve shapes for depths of 10 mm, 30 mm and 50 mm are very similar. S_{21} decreases with tumor depth, with maximum values of –58.1 dB at d=10 mm, -68.3 dB at d=30 mm and –75.2 dB at d=50 mm. Therefore, it

appears feasible to detect a 4.8 mm long and 1.6 mm wide ellipsoidal tumor at a depth of 5 cm. To further study detection capabilities, the tumor size is decreased (case 4). Fig. 5 suggests the feasibility of detecting ellipsoidal tumors with axial lengths of 3 mm and greater.

The effects of changing tumor orientation are examined in Figs. 6 and 7. S_{21} increases as the tumor rotates from 0 to 45 degrees relative to the xy axes of the antenna. S_{21} decreases as the tumor rotates in the xz plane from 0 to 90 degrees.

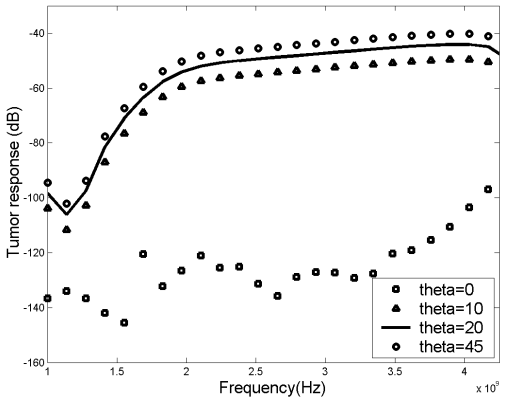

Fig. 6 Change in S_{21} with θ (case 5)

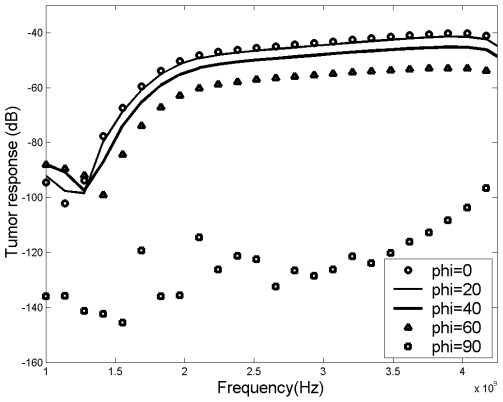

Fig. 7 Change in S_{21} with ϕ (case 6).

Conclusions

A significant cross-polarized response from spherical and ellipsoidal tumors is observed over the band from 2 to 4.3 GHz. This response is obtained with various tumor depths, orientations and locations. It appears advantageous to scan the antenna through various locations and orientations to avoid missing a tumor. Further study with more realistic models of the breast and tumor is required.

References

[1] E.C. Fear, S.C. Hagness, P.M. Meaney, M. Okoniewski and M.A. Stuchly, "Near-field imaging for breast tumor detection," *IEEE Microw. Mag.*, vol. 3, March 2002, pp. 48-56.

[2] S. C. Hagness, A. Taflove, and J. E. Bridges, "Three-dimensional FDTD analysis of a pulsed microwave confocal system for breast cancer detection: design of an antenna-array element," *IEEE Trans. Antennas Propag.*, vol. 47, May 1999, pp. 783-791,

[3] C.-C. Chen, M.B. Higgins, K. O'Neill, and R. Detsch, "Ultrawide-bandwidth fully-polarimetric ground penetrating radar classification of subsurface unexploded ordnance" *IEEE Trans. Geosci. Remote Sensing*, vol. 39, June 2001, pp. 1221-1230.

[4] B.M. Kolundzija, J.S. Ognjanovic, and T.K. Sarkar, *WIPL-D Electromagnetic modeling of composite metallic and dielectric structures,* Artech House, Boston, 2000.